

PAPER • OPEN ACCESS

## Phaseless tomographic inverse scattering in Banach spaces

To cite this article: C. Estatico *et al* 2016 *J. Phys.: Conf. Ser.* **756** 012010

View the [article online](#) for updates and enhancements.

### Related content

- [Uniqueness of a one-dimensional phase retrieval problem](#)  
Michael V Klibanov and Vladimir G Kamburg
- [Uniqueness results on phaseless inverse acoustic scattering with a reference ball](#)  
Deyue Zhang and Yukun Guo
- [A multi-frequency MRCIS algorithm with phaseless data](#)  
Zheng Hu, Li Lianlin and Li Fang



**IOP | ebooks™**

Bringing you innovative digital publishing with leading voices to create your essential collection of books in STEM research.

Start exploring the collection - download the first chapter of every title for free.

# Phaseless tomographic inverse scattering in Banach spaces

C. Estatico<sup>1</sup>, A. Fedeli<sup>2</sup>, M. Pastorino<sup>2</sup>, A. Randazzo<sup>2</sup>, E. Tavanti<sup>2</sup>

<sup>1</sup>Department of Mathematics, University of Genoa, Via Dodecaneso 35, I-16146 Genoa, Italy.

<sup>2</sup>Department of Electrical, Electronic, Telecommunication Engineering, and Naval Architecture, University of Genoa, Via Opera Pia 11A, I-16145, Genoa, Italy.

E-mail: [estatico@dima.unige.it](mailto:estatico@dima.unige.it)

**Abstract.** In conventional microwave imaging, a hidden dielectric object under test is illuminated by microwave incident waves and the field it scatters is measured in magnitude and phase in order to retrieve the dielectric properties by solving the related non-homogenous Helmholtz equation or its Lippmann-Schwinger integral formulation. Since the measurement of the phase of electromagnetic waves can be still considered expensive in real applications, in this paper only the magnitude of the scattering wave fields is measured in order to allow a reduction of the cost of the measurement apparatus. In this respect, we firstly analyse the properties of the phaseless scattering nonlinear forward modelling operator in its integral form and we provide an analytical expression for computing its Fréchet derivative. Then, we propose an inexact Newton method to solve the associated nonlinear inverse problems, where any linearized step is solved by a  $L^p$  Banach space iterative regularization method which acts on the dual space  $L^{p^*}$ . Indeed, it is well known that regularization in special Banach spaces, such as  $L^p$  with  $1 < p < 2$ , allows to promote sparsity and to reduce Gibbs phenomena and over-smoothness. Preliminary results concerning numerically computed field data are shown.

## 1. Introduction

Electromagnetic imaging methods based on inverse scattering analysis [1], especially those working at microwave frequencies, are acquiring an ever growing importance for non-destructive testing in several real applicative fields, ranging from civil, industrial to biomedical engineering [2–6]. Basically, information provided by microwave scattering phenomena measured outside an unknown dielectric object under test are used to characterize the spatial distributions of its dielectric properties (e.g., dielectric permittivity, electric conductivity, and magnetic permeability). The main advantage of microwave imaging is its intrinsic low invasivity with respect, for instance, to X-ray tomographic apparatuses. On the other hand, non-destructive imaging by microwave inverse scattering turns out to be an extremely complicated problem, due to a high non-linear response and a severe ill-positioning of the governing equations that relate the scattered electromagnetic field to the dielectric properties of the scatterer. Hence, regularization methods are required to overcome the ill-posedness and reduce both instability and noise-amplification in the restoration process [7,8].

In conventional inverse scattering, a large amount of information about the scattered field is acquired, that is, a large collection of measured electromagnetic fields by multi-view/illumination and multi-frequency systems, where any measure generally involves both wave magnitude and phase. Although this large set of data can be useful to improve the quality of the whole imaging apparatuses, since it allows for a better restoration of the dielectric properties of the unknown scatterer, its acquisition can be still expensive. A possible way to reduce the whole costs of the imaging apparatuses is to acquire magnitude-only data. Clearly, in this case it is also necessary to employ

<sup>1</sup> E-mail: [estatico@dima.unige.it](mailto:estatico@dima.unige.it). The work of C. Estatico is partly supported by PRIN 2012 N. 2012MTE38N.

<sup>2</sup> E-mail: [alessandro.fedeli@edu.unige.it](mailto:alessandro.fedeli@edu.unige.it); [matteo.pastorino@unige.it](mailto:matteo.pastorino@unige.it); [andrea.randazzo@unige.it](mailto:andrea.randazzo@unige.it); [emanuele.tavanti@edu.unige.it](mailto:emanuele.tavanti@edu.unige.it).



inverse scattering procedures that require only information about the magnitude of the scattered field or techniques for approximating the missing information about the phase [9–14].

In this work, a fully phaseless inverse scattering model is introduced and implemented. Basically, neither direct measurements nor indirect estimations of the phase of the electromagnetic scattered field are required to derive the dielectric parameters of the object under test. In this respect, the nonlinear Lippmann-Schwinger integral formulation of the phaseless forward scattering model has been analysed, in order to derive a procedure for its inversion. More specifically, the non-linear phaseless inverse scattering integral equation has been solved by an inexact-Newton method, where the solution of any linearized equation is computed by an iterative regularization algorithm for ill-posed linear functional equations in  $L^p$  Banach spaces [15–18]. We recall that regularization in  $L^p$  Banach spaces, for  $1 < p < 2$ , is able to promote sparsity and reduce the over-smoothing effects arising in conventional regularization in Hilbert space  $L^2$ . Heuristically, regularization in  $L^p$ , with  $1 < p < 2$ , is based on a convex and smooth minimization which approximates the minimization on the non-smooth  $L^1$  space, which is well-known to be the basic framework of the so-called “sparse recovering”. This way, since the  $L^p$ -norm is differentiable (as well as the  $L^2$ -norm), the computation in  $L^p$ , with  $1 < p < 2$ , is cheaper than dealing with  $L^1$ -norm, which is not differentiable, but the sparsity is still promoted [15]. A first numerical validation shows that the proposed low-cost phaseless microwave inverse scattering method in Banach space improves the results of the corresponding phaseless method developed in the standard Hilbert space.

The paper is organized as follows. In Section 2, the considered electromagnetic is described. The developed inversion procedure is detailed in Section 3. Preliminary numerical results are shown in Section 4. Finally, conclusions are drawn in Section 5.

## 2. The phaseless tomographic microwave inverse scattering model

By assuming cylindrical scatterers and transverse-magnetic illuminations, the electromagnetic scattering phenomena can be described by the following two-dimensional and scalar Lippmann-Schwinger integral equation [1]

$$E_{scat}(\mathbf{r}) = \iint_{D_{inv}} G_0(\mathbf{r}, \boldsymbol{\xi}) c(\boldsymbol{\xi}) E_{tot}(\boldsymbol{\xi}) d\boldsymbol{\xi}, \quad \mathbf{r} \in D_{obs}. \quad (1)$$

Here  $D_{obs}$  is the observation domain where the samples of the electric field are collected,  $E_{inc}$  is a known incident electric field,  $E_{tot}$  is the total electric field,  $c = \epsilon_r - 1$  is the contrast function (being  $\epsilon_r$  the complex relative dielectric permittivity),  $G_0$  is the free space two-dimensional Green’s function [19],  $D_{inv}$  is the investigation domain where the unknown scatterer is placed, and  $E_{scat} = E_{tot} - E_{inc}$  denotes the scattered electric field. Equation (1) is known as data equation and belongs to the first kind Fredholm integral equations class, hence it is well known to be ill posed. Along with it, we need another one, known as state equation, relating incident and total electric field inside the scatterer

$$E_{inc}(\mathbf{r}) = E_{tot}(\mathbf{r}) - \iint_{D_{inv}} G_0(\mathbf{r}, \boldsymbol{\xi}) c(\boldsymbol{\xi}) E_{tot}(\boldsymbol{\xi}) d\boldsymbol{\xi}, \quad \mathbf{r} \in D_{inv}. \quad (2)$$

Equations (1) and (2) are discretized by using the method of moments [20]. In particular,  $D_{inv}$  is partitioned in  $N$  pixels with centers  $\mathbf{r}_n^{inv}$ ,  $n = 1, \dots, N$ , where both the field and the contrast function are assumed to be constant, and the external electric field is collected in  $M$  measurements point  $\mathbf{r}_m^{obs}$ ,  $m = 1, \dots, M$ , belonging to  $D_{obs}$ . Consequently, the following discretized form is obtained (see for example [1] for the details about the involved quantities)

$$\begin{aligned} \mathbf{E}_{scat}^{ext} &= \mathbf{G}^e \text{diag}(\mathbf{c}) \mathbf{E}_{tot}^{int} \\ \mathbf{E}_{inc}^{int} &= [\mathbf{I} - \mathbf{G}^i \text{diag}(\mathbf{c})] \mathbf{E}_{tot}^{int}. \end{aligned} \quad (3)$$

Combining the two equations in (3), we get the following compact matrix equation

$$\mathbf{E}_{scat}^{ext} = \mathbf{G}^e \text{diag}(\mathbf{c}) [\mathbf{I} - \mathbf{G}^i \text{diag}(\mathbf{c})]^{-1} \mathbf{E}_{inc}^{int} = \mathbf{G}^e \text{diag}(\mathbf{c}) \mathbf{E}_{tot}^{int}(\mathbf{c}) = \mathbf{F}(\mathbf{c}). \quad (4)$$

This basic formulation involves both amplitude and phase components in  $\mathbf{E}_{scat}^{ext}$ . However, in this paper we assume that only magnitude measurements are available, i.e., we assume that the data we dispose are only those related to  $|E_{scat}(\mathbf{r})|^2$ . Therefore, the scattering model in (4) is modified as follows

$$\mathbf{P}_{scat}^{ext} = \bar{\mathbf{F}}(\mathbf{c}) \circ \mathbf{F}(\mathbf{c}) = \mathbf{F}_p^{cplx}(\mathbf{c}) = \mathbf{F}_p^{cplx}(\mathbf{T}\mathbf{x}) = \mathbf{F}_p(\mathbf{x}). \quad (5)$$

Here  $\mathbf{P}_{scat}^{ext}$  is an array containing the values of  $|E_{scat}(\mathbf{r})|^2$  in the measurement points, the upper bar denotes the element-wise complex conjugate, and  $\circ$  denotes the Hadamard product. In order to obtain a real-valued unknown, we rewrite our problem in terms of  $\mathbf{x} = [Re(\mathbf{c}^t) Im(\mathbf{c}^t)]^t$ . Consequently, the transformation  $\mathbf{c} = \mathbf{T}\mathbf{x} = [\mathbf{I} \ j\mathbf{I}]\mathbf{x}$  is applied into the model in (5) in order to obtain the final forward operator  $\mathbf{F}_p$ .

### 3. The solution of the inverse problem in Banach spaces via quasi-Newton schemes

A successful algorithm to solve the conventional formulation (4) is the inexact-Newton scheme with regularizing Landweber method inside  $L^p$  Banach spaces, with  $1 < p < 2$  [15]. Due to its flexibility, we choose to apply it also to cope with the proposed phaseless model equation (5). Such approach can be summarized by the following steps ( $n$  and  $l$  are indexes for outer Newton and inner Landweber loops, respectively):

- I) Initialize the procedure with an initial guess  $\mathbf{x}_0$ . A modified back-propagation procedure is employed to find a suitable non-null value.
- II) Linearize (5) around the current estimate  $\mathbf{x}_n$ . The following linear system is obtained

$$\mathbf{F}'_p(\mathbf{x}_n) \boldsymbol{\delta} = \mathbf{P}_{scat}^{ext} - \mathbf{F}_p(\mathbf{x}_n) = \mathbf{r}_n. \quad (6)$$

Indeed, through the Taylor expansion of (4), that is,

$$\begin{aligned} \mathbf{F}(\mathbf{c} + d\mathbf{c}) &= \\ \mathbf{G}^e \text{diag}(\mathbf{c}) \mathbf{E}_{tot}^{int}(\mathbf{c}) + \mathbf{G}^e [\mathbf{I} - \text{diag}(\mathbf{c}) \mathbf{G}^i]^{-1} \text{diag}(d\mathbf{c}) \mathbf{E}_{tot}^{int}(\mathbf{c}) + O[\text{diag}(d\mathbf{c})^2 \mathbf{E}_{inc}^{int}], \end{aligned} \quad (7)$$

the Fréchet derivative of the forward operator in (5) can be explicitly computed as

$$\mathbf{F}'_p(\mathbf{x}) = 2Re\{\text{diag}[\bar{\mathbf{F}}(\mathbf{x})] \mathbf{F}'(\mathbf{x}) \mathbf{T}\} \quad (8)$$

where  $\mathbf{F}'$  is the Fréchet derivative of the complex-data problem in (4) [16].

- III) Approximate the solution of (6) by the following Landweber iterations for the minimization of the residual  $\frac{1}{2} \|\mathbf{F}'_p(\mathbf{x}_n) \boldsymbol{\delta} - \mathbf{r}_n\|_{L^p}^2$  in  $L^p$  Banach space ( $\boldsymbol{\delta}_0 = \hat{\boldsymbol{\delta}}_0 = \mathbf{0}$ )

$$\begin{aligned}\widehat{\boldsymbol{\delta}}_{l+1} &= \widehat{\boldsymbol{\delta}}_l - \beta \mathbf{F}_p'^*(\mathbf{x}_n) \mathbf{J}_p[\mathbf{F}_p'(\mathbf{x}_n) \widehat{\boldsymbol{\delta}}_l - \mathbf{r}_n] \\ \boldsymbol{\delta}_{l+1} &= \mathbf{J}_q(\widehat{\boldsymbol{\delta}}_{l+1})\end{aligned}\tag{9}$$

Here  $1 < p < 2$ ,  $\mathbf{F}_p'^*(\mathbf{x}_n)$  is the adjoint operator of  $\mathbf{F}_p'(\mathbf{x}_n)$ ,  $\beta \in (0, 2\|\mathbf{F}_p'(\mathbf{x}_n)\|_2^{-2})$  is the relaxation coefficient,  $q = p/(p - 1)$  is the Holder conjugate of  $p$ ,  $\mathbf{J}_p: L^p \rightarrow L^q$  and  $\mathbf{J}_q: L^q \rightarrow L^p$  are the normalized duality maps of the  $L^p$  and  $L^q$  Banach spaces respectively. We recall that the normalized duality map  $\mathbf{J}_p(s) = \partial\left(\frac{1}{2}\|s\|_{L^p}^2\right)$  of  $L^p$  is explicitly computable as  $\mathbf{J}_p(s) = \|s\|_{L^p}^{2-p}|s|^{p-1}\text{sign}(s)$ , where  $\text{sign}(s) = e^{j \arg(s)}$  if  $s \neq 0$  and  $\text{sign}(s) = 0$  [16] (please notice that, when  $p = 2$ , then  $\mathbf{J}_2(s) = s$ ).

The iterations are stopped if a maximum number of iterations  $l_{max}$  is reached or if the relative variation of the residuals between two consecutive iterations is below a fixed threshold  $\varepsilon_L$ . Set  $\boldsymbol{\delta}$  as the last computed inner iteration  $\boldsymbol{\delta}_{l+1}$ .

IV) Update the solution with

$$\mathbf{x}_{n+1} = \mathbf{x}_n + \boldsymbol{\delta}.\tag{10}$$

V) Iterate steps II-IV until a maximum number  $n_{max}$  of iterations is reached or a predefined stopping rule is satisfied.

The Landweber scheme (9) is proven to be an effective regularization algorithm. We remark that the iterations defined in the equation of (9) are computed in the dual space of  $L^p$  [15].

#### 4. A preliminary numerical validation

The developed approach has been preliminarily tested by using numerical data. We focus on a square investigation area of side 1 m, which has been partitioned into  $N = 1600$  square cells. The target is a rectangular cylinder with relative dielectric permittivity  $\varepsilon_r = 2$  and with the dimension shown in Figure 1.

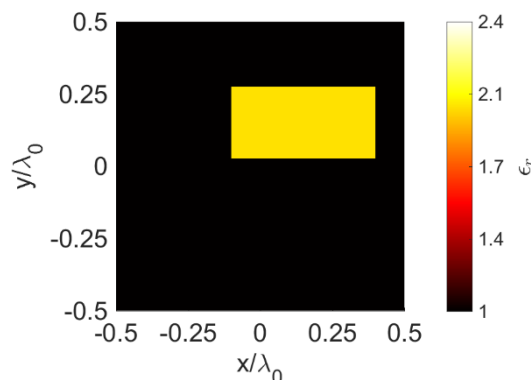


Figure 1. Distribution of the dielectric permittivity in the investigation domain used for tests.

The measurement points are  $M = 91$ , uniformly located on a circumference of radius 1.5 m and centered in (0,0). The investigation area is illuminated by  $V = 8$  line-current sources (the working frequency is 300 MHz). The values of  $V$  and  $M$  have been chosen to properly sample the field. A zero mean value white Gaussian noise with  $SNR = 25$  dB has been added to the simulated field data in order to emulate real operating conditions. The maximum numbers of outer and inner iterations are equal to  $n_{max} = 20$  and  $l_{max} = 10$ , respectively, with  $\varepsilon_L = 0.01$ . Figure 2 shows the results returned by using  $p = 1.4$  and  $p = 2.0$ ; the last one corresponds to the standard Hilbert space inversion.

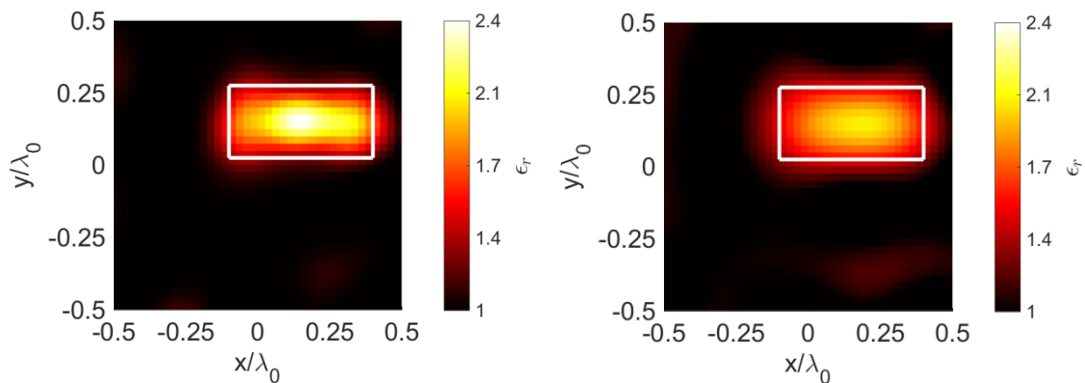


Figure 2. Reconstruction with phaseless measurements. Left:  $p = 1.4$ ; Right:  $p = 2.0$ . The mean reconstruction relative errors on the object are: 0.0731 (left) and 0.1005 (right).

For  $p = 1.4$ , the target is located and shaped correctly with a clean background. However, it should be noted that the relative dielectric permittivity of the scatterer is overestimated. On the contrary, for  $p = 2.0$ , the shape is more irregular and artefacts are present in the background. For comparison purposes, Figure 3 reports the results obtained by using the full complex data (that is, both magnitude and phase) with the procedure developed in [16].

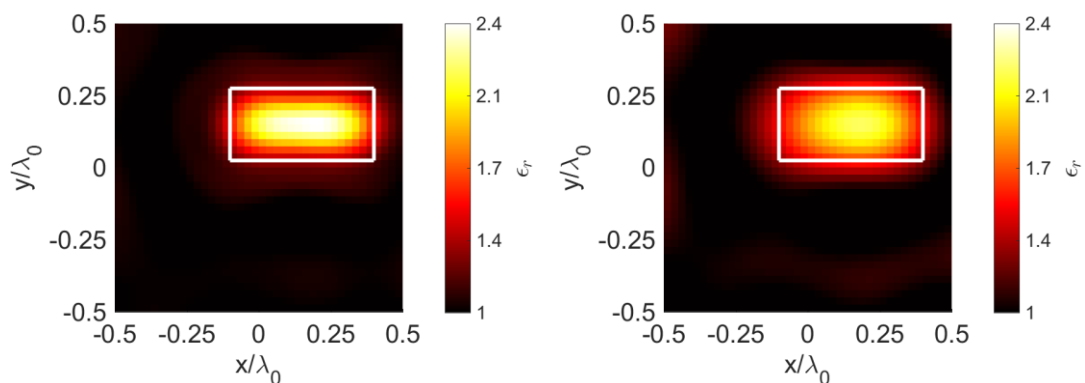


Figure 3. Reconstruction with full complex measurements. Left:  $p = 1.4$ ; Right:  $p = 2.0$ . The mean reconstruction relative errors on the object are: 0.0605 (left) and 0.0692 (right).

Clearly, the availability of the phase allows a better reconstruction. For  $p = 1.4$ , the scatterer is again located correctly with a clean background; the overestimation phenomena still persists, although now it is weaker than in the previous case. For  $p = 2.0$ , considerations about the phaseless case can be proposed again here. We can assert that our phaseless approach exhibits interesting reconstruction capabilities and flexibility due to the tunable  $p$  parameters, although the inversion performed with complex (and expensive) measurements has a higher quality.

## 5. Conclusions

A fully phaseless microwave imaging method has been presented in this paper. The developed approach employs an efficient inversion procedure in the framework of the regularization in  $L^p$  Banach spaces, which has been found to provide better results than the corresponding conventional Hilbert space regularization methods. Accordingly, the preliminary numerical validation shows that the proposed phaseless microwave inverse scattering technique in Banach spaces is able to improve the results of the corresponding phaseless method developed in the standard Hilbert space. Clearly, as expected, the method provides worse results than the corresponding approach working with full complex data. However, at least in these preliminary tests, the quality of the restorations obtained by

means of the proposed phaseless technique is still quite good. A possible future improvement is to adopt a multi-scaling approach, which is known to be a valid instrument in microwave imaging [21].

## References

- [1] Pastorino M 2010 *Microwave imaging* (Hoboken, N.J.: Wiley)
- [2] Benedetto A and Pajewski L 2015 *Civil Engineering Applications of Ground Penetrating Radar* (Cham: Springer International Publishing)
- [3] Hossain M D, Mohan A S and Abedin M J 2013 Beamspace time-reversal microwave imaging for breast cancer detection *IEEE Antennas Wirel. Propag. Lett.* **12** 241–4
- [4] Mohammed B J, Abbosh A M, Mustafa S and Ireland D 2014 Microwave System for Head Imaging *IEEE Trans. Instrum. Meas.* **63** 117–23
- [5] Pastorino M, Randazzo A, Fedeli A, Salvadè A, Poretti S, Maffongelli M, Monleone R and Lanini M 2015 A microwave tomographic system for wood characterization in the forest products industry *Wood Mater. Sci. Eng.* **10** 75–85
- [6] Kharkovsky S and Zoughi R 2007 Microwave and millimeter wave nondestructive testing and evaluation - Overview and recent advances *IEEE Instrum. Meas. Mag.* **10** 26–38
- [7] Bertero M and Boccacci P 1998 *Introduction to inverse problems in imaging* (Bristol, UK: IOP Publishing)
- [8] Kaltenbacher B 1997 Some Newton-type methods for the regularization of nonlinear ill-posed problems *Inverse Probl.* **13** 729–53
- [9] Costanzo S, Di Massa G, Pastorino M and Randazzo A 2015 Hybrid Microwave Approach for Phaseless Imaging of Dielectric Targets *IEEE Geosci. Remote Sens. Lett.* **12** 851–4
- [10] Zheng H, Wang M-Z, Zhao Z and Li L 2010 A novel linear EM reconstruction algorithm with phaseless data *Prog. Electromagn. Res. Lett.* **14** 133–46
- [11] Lianlin Li, Hu Zheng and Fang Li 2009 Two-Dimensional Contrast Source Inversion Method With Phaseless Data: TM Case *IEEE Trans. Geosci. Remote Sens.* **47** 1719–36
- [12] D’Urso M, Belkebir K, Crocco L, Isernia T and Litman A 2008 Phaseless imaging with experimental data: facts and challenges *J. Opt. Soc. Am. A* **25** 271
- [13] Caorsi S, Massa A, Pastorino M and Randazzo A 2003 Electromagnetic detection of dielectric scatterers using phaseless synthetic and real data and the memetic algorithm *IEEE Trans. Geosci. Remote Sens.* **41** 2745–53
- [14] Franceschini G, Donelli M, Azaro R and Massa A 2006 Inversion of Phaseless Total Field Data Using a Two-Step Strategy Based on the Iterative Multiscaling Approach *IEEE Trans. Geosci. Remote Sens.* **44** 3527–39
- [15] Schuster T, Kaltenbacher B, Hofmann B and Kazimierski, K 2012 *Regularization methods in Banach spaces* (Berlin: De Gruyter)
- [16] Estatico C, Pastorino M and Randazzo A 2012 A novel microwave imaging approach based on regularization in  $L_p$  Banach spaces *IEEE Trans. Antennas Propag.* **60** 3373–81
- [17] Estatico C, Fedeli A, Pastorino M and Randazzo A 2015 A multifrequency inexact-Newton method in  $L_p$  Banach spaces for buried objects detection *IEEE Trans. Antennas Propag.* **63** 4198–204
- [18] Estatico C, Fedeli A, Pastorino M and Randazzo A 2015 Buried object detection by means of a  $L_p$  Banach-space inversion procedure *Radio Sci.* **50** 41–51
- [19] Pastorino M, Raffetto M and Randazzo A 2014 Two-Dimensional Green’s Function for Scattering and Radiation Problems in Elliptically-Layered Media *IEEE Trans. Antennas Propag.* **62** 2071–80
- [20] Harrington R 1993 *Field Computation by Moment Methods* (Piscataway, NJ: IEEE Press)
- [21] Oliveri G, Lizzi L, Pastorino M and Massa A 2012 A nested multi-scaling inexact-Newton iterative approach for microwave imaging *IEEE Trans. Antennas Propag.* **60** 971–83